Highlights

- With the use of qpCR we identified the NMDA receptor composition in different brain areas
- Using Double-fluorescent in situ hybridization we demonstrated that TH+ cells contain the NMDA Glun2C subunit
- Using deep brain stimulation of the dorsal raphe and small interfering RNA we demonstrate that the reward signal is carried to VTA neurons through activation of Glun2C NMDA receptors.

17 **Title: Dorsal raphe stimulation relays a reward signal to the ventral tegmental area via**

18 **GluN2C NMDA receptors**

19

20 **Running tittle: VTA NMDA GluN2C subunit relays the reward signal**

21 **Authors :** Hernandez, Giovanni [1]; Kouwenhoven, Willemieke M[2]; Poirier Emmanuelle[1]; Lebied Karim[1],

22 Lévesque, Daniel[3]; Rompré, Pierre-Paul[1]

23 (1) Département de neurosciences (Faculté de médecine), (2) Département de pharmacologie et

24 physiologie (Faculté de médecine), (3) Faculté de Pharmacie, Université de Montréal, Montréal, QC.

25

26 Number of pages :

27 - Number of pages

28 - ☐ Number of figures, tables, multimedia, and 3D models (separately)

29 - ☐ Number of words for

30 - o abstract:257

31 - o Introduction: 877

32 - o Discussion: 1516

33 - **Acknowledgments** The present research was supported by NSERC grant # 119057 to

34 Pierre-Paul Rompré, Herbert H. Jasper fellowship to Giovanni Hernandez, CIHR

35 operating grant #130407 to Daniel Lévesque.

- **Disclosure:** The authors confirm that they don't have a conflict of interest related to these studies.

Corresponding Author(s): Hernandez, Giovanni. Mailing address: Neuroscience Department Douglas Research Hospital, 6875 Boulevard LaSalle. E-2107, Perry Pavilion.Montréal, QC H4H 1R3. E-mail : giovanni.hernandez.comtl@ssss.gouv.qc.ca. Phone number 514-8308293

Rompré, Pierre-Paul. Mailing address Département de Neurosciences Université de Montréal Pavillon Paul-G. Desmarais, 2960 Chemin de la Tour. Montréal, QC H3T 1N8. E-mail : pierre-paul.rompre@umontreal.ca Phone number : 514-3436111 ext 35351

Keywords: NMDA receptors, GluN2C, Grin2c transcript, Dorsal Raphe, Dopamine, Glutamate, Reward

Abstract:

Background: Glutamate relays a reward signal from the dorsal raphe (DR) to the ventral tegmental area (VTA). However, the role of the different subtypes of N-methyl-D-aspartate (NMDA) receptors is complex and not clearly understood. Therefore, we measured NMDA receptors subunits expression in limbic brain areas. In addition, we studied the effects of VTA down-regulation of GluN2C NMDA receptor on the reward signal that arises from DR electrical stimulation.

Methods: Using qPCR, we identified the relative composition of the different Grin2a-d subunits of the NMDA receptors in several brain areas. Then, we used fluorescent *in situ* hybridization (FISH) to evaluate the colocalization of Grin2c and tyrosine hydroxylase (TH) mRNA in VTA neurons. To assess the role of GluN2C in brain stimulation reward; we downregulated this receptor using small interfering RNA (siRNA) in rats self-stimulating for electrical pulses delivered to the DR. To delineate further the specific role of GluN2C in relaying the reward signal, we pharmacologically altered the function of VTA NMDA receptors by bilaterally microinjecting the NMDA receptor antagonist PPPA.

Results: We identified GluN2C as the most abundant subunit of the NMDA receptor expressed in the VTA. FISH revealed that about 50% of TH-positive neurons colocalize with Grin2c transcript. siRNA manipulation produced a selective down-regulation of the GluN2C protein subunit and a significant reduction in brain stimulation reward. Interestingly, PPPA enhanced brain stimulation reward, but only in rats that received the nonactive RNA sequence.

Conclusion: The present results suggest that VTA glutamate neurotransmission relays a reward signal initiated by DR stimulation by acting on GluN2C NMDA receptors.

Introduction

The dorsal raphe nucleus (DR) plays a key role in the transmission of a reward signal [1–5]. It contains a heterogeneous group of neurons that send one of the highest projection density to the ventral tegmental area (VTA) [6], the origin of dopamine (DA) pathways implicated in reward and motivation [7–12]. Studies combining psychophysical methods with brain stimulation reward (BSR) revealed that activation of DR neurons triggers a strong reward signal [13,14] that travels along axons linking the DR to the VTA [3]; the combination of BSR with in vivo electrophysiology also showed that the DR reward signal activates a subpopulation of VTA DA-like neurons and that the magnitude of this activation is proportional to the magnitude of the reward signal [3,15]. The DR contains a large number of serotoninergic neurons [16], but it also contains glutamatergic, nitric oxide synthase, GABAergic and dopaminergic neurons [17]. The use of paired-pulse stimulation strongly suggests that serotonergic DR neurons do not carry the reward signal because the refractory periods of the reward-relevant neurons that linked DR to VTA are incompatible with those of serotoninergic neurons [3,18,19]. Indeed, more recent optogenetic studies revealed that the selective activation of DR glutamatergic and their VTA terminals triggers a reward signal [1,2,20]. Glutamate-containing terminals established asymmetrical synapses with DA neurons [2,21], and VTA glutamate release stimulates DA activity leading to the enhancement of extracellular DA in the nucleus accumbens, a limbic region that plays a key role in reward and motivation [2,22].

According to data from Qi et al. (2014), glutamate ionotropic AMPA receptors participate in the transmission of the DR reward signal to VTA mesoaccumbens DA neurons; however, several well-known characteristics of the interaction between glutamate and DA in the VTA suggest an important contribution of glutamate NMDA receptor subtypes (NMDAR). Activation of VTA NMDARs makes DA neurons to switch from a tonic, single-spike irregular firing pattern to a phasic burst firing pattern

92 (Chergui et al., 1993a; Grace & Bunney, 1984; Hyland, Reynolds, Hay, Perk, & Miller, 2002; Johnson,
93 Seutin, & North, 1992; P. G. Overton & Clark, 1997; Parker et al., 2010; Zweifel et al., 2009), a firing
94 mode associated with an increased DA release and transmission of a reward signal [26,27]. But, besides
95 this firing transition role relevant to reward, VTA glutamate also plays a role in maintaining a DA
96 inhibitory drive (Grace et al., 2007). For example, pharmacological blockade of VTA NMDARs was shown
97 to stimulate DA impulse flow and release, induce reward, and facilitate reward search [5]; an opposite
98 effect is observed following the blockade of VTA NMDRs. The enhancement of DA neurotransmission
99 and reward may occur via the attenuation of the tonic inhibitory afferent inputs to DA, increasing the
100 probability that DA neurons fire in a burst mode. The opposite modulation of DA by glutamate may be
101 explained by its action in different VTA neuronal populations expressing different subtypes of NMDAR.
102 This hypothesis predicts that activation of a given subtype(s) potentiates DA burst firing and DA release,
103 while activation of different subtype(s) increases the inhibitory drive to DA neurons. This idea is
104 supported by data mentioned above and others showing that both activation and blockade of VTA
105 NMDARs increase DA burst firing (French et al., 1993), accumbens DA release (Karreman et al., 1996;
106 Westerink et al., 1996; Mathé et al., 1998; Kretschmer, 1999), and stimulate forward locomotion
107 (Kretschmer, 1999; Cornish et al., 2001). Rodents also readily learn to directly self-administer the non-
108 selective NMDAR antagonists, AP-7, into the VTA (David et al., 1998), showing that NMDAR blockade can
109 have positive, rewarding properties on its own.

110 NMDARs are formed by tetrameric complexes composed of two obligatory GluN1 subunits that
111 cluster with GluN2 and/or GluN3 subunits [28,29]. In a previous study of our group, we reported that
112 down-regulation of GluN1 subunit protein in VTA neurons, which produces a non-selective reduction in
113 NMDAR expression, results in a specific attenuation of reward induced by DR electrical stimulation [30].
114 However, we could not identify the GluN1 subunit partner because a similar downregulation of the
115 GluN2A or GluN2D subunit failed to alter brain stimulation reward [30]; Moreover, selective

116 pharmacological blockade of VTA GluN2B subunits did not affect the reward signal arising from the DR
117 [5].

118 Here, we first report that Grin2c mRNA is expressed in the VTA in higher concentration than other
119 Grin2 transcripts (a, b, or d) and colocalizes within tyrosine hydroxylase positive (TH+) and negative (TH-)
120 neurons, and second that selective downregulation of VTA NMDAR containing GluN2C subunits leads to
121 a specific attenuation of the reward signal initiated by DR electrical stimulation.

122

123 **Materials and Methods**

124 **Subjects and surgery**

125 Twenty-two (22) male Long-Evans rats (Charles River, St-Constant, QC) weighing between 350-
126 400 g at the time of surgery were used. Rats were individually housed in a temperature- and humidity-
127 controlled room with a 12-h light-dark cycle (lights on at 06:00 h) and *ad libitum* access to food and
128 water. After a minimum 7-day period of acclimatization to the housing, environment rats were
129 anesthetized with isoflurane (2.5-3.5% O2, 0.6 L/min) and stereotaxically implanted according to the
130 coordinates of Paxinos and Watson (2007) with 26-gauge guided cannulae (HRS Scientific, Montreal,
131 Canada) aimed bilaterally at the VTA (-5.5 AP, 3.2 ML at an angle of 18 °, 6.5 DV from the skull surface)
132 and a monopolar stainless steel monopolar electrode aimed at the DR (-7.6 AP, 0 ML, 6.6 DV from the
133 skull surface). Detailed surgical procedures can be found in Bergeron and Rompré (2013). All procedures
134 were approved by the Animal Care and Use Committee of the Université de Montréal in accordance
135 with the guidelines of the Canadian Council on Animal Care.

136 **siRNAs and Drugs**

137 Downregulation of selective NMDAR subunit expression was achieved using a pre-validated small
138 interfering RNA (siRNA) sequence against the rat glutamate ionotropic receptor NMDA type subunit 2C
139 (Grin2c) mRNA, which encodes the GluN2C protein subunit (Silencer™ select pre-designed siRNA #
140 4390771, siRNA ID s127815, ThermoFisher Scientific) and a nonactive RNA sequence (Silencer™ select
141 negative control #4390844, ThermoFisher Scientific). The deprotected, duplexed, desalted siRNA was
142 mixed with a cationic lipid transfection carrier N-[1-(2,3-Dioleoyloxy)propyl]-N, N, N-trimethyl-
143 ammonium methylsulfate (DOTAP) (Roche Applied Sciences, Indianapolis, IN), which showed high
144 efficacy for *in vivo* transfection [31]. The final solution contained 10 µg of active or inactive siRNA and 1
145 µg of DOTAP per µl.

146 PPPA ((2R, 4S) -4- (3-phosphatophores) -2-piperidinecarboxylic acid), a competitive GluN2A-
147 favored NMDAR antagonist (Tocris, Ellisville, MI, USA), was dissolved in 0.9% sterile saline and stored
148 frozen in 40–50 µl aliquots. Drug solutions were thawed just before testing and used only once. PPPA
149 was injected into VTA at a dose of 0.825 nmol/0.5µl/side, as previously described [5,30,32].

150 **Self-stimulation training**

151 Each rat was trained to nose-poke for a 0.4-sec train of cathodal, rectangular, constant-current
152 pulses, 0.1 msec in duration, delivered at a frequency of 98 Hz. For a detailed shaping procedure, see
153 [5]. Once the rat nose-poked consistently for currents between 125 and 400 µA, a rate vs. pulse-
154 frequency curve was obtained by varying the stimulation frequency across trials over a range that drove
155 the number of rewards earned from maximal to minimal levels. The stimulation frequency was
156 decreased from trial to trial by approximately 0.05 log10. Each trial for obtaining the rate-frequency
157 sweep lasted for 55 s, followed by a 15 s inter-trial interval during which stimulation was not available.
158 The beginning of each trial was signaled by five trains of non-contingent priming stimulation delivered at
159 a rate of 1 per second. Four sweeps were run daily, and the first sweep was considered a warm-up and

160 discarded from the analysis. The data relating to the rate-frequency was fitted to a sigmoid described by
161 the following equation y=Min+((Max-Min))/(1+[10]^((x50-x)*p)) where Min is the lower asymptote,
162 Max is the upper asymptote, x50 is the position parameter denoting the frequency at which the slope of
163 the curve is maximal, and p determines the steepness of the sigmoid curve. The resulting fit was used to
164 derive an index of reward defined as the pulse-frequency sustaining a half-maximal rate of responding
165 (M50). Self-stimulation behavior was considered stable when the M50 values varied less than 0.1 log
166 unit for three consecutive days.

167 Prior to the siRNA injections or drug administration, sterile 0.9% saline was microinjected into the
168 VTA to habituate the animals to the injection procedure. Bilateral injections were performed by
169 inserting an injection cannula (Model C315I HRS Scientific, Montreal, Canada) that extended 2 mm
170 beyond the tip of the guide cannula. The injection cannula was connected to a 5 µl Hamilton
171 microsyringe via polyethylene tubing. A total volume of 0.5 µl was injected into each hemisphere
172 simultaneously over a 60-s period. The rate of delivery was controlled by an infusion pump (Harvard
173 Instruments, Holliston, MA). The injection cannulae were left in place for an additional 60 s to allow
174 diffusion into the tissue. After microinjection, the subjects were put into the operant boxes and allowed
175 to self-stimulate. The results of this test were not included in the analysis. Baseline data were collected
176 one week after this first saline microinjection. Once a stable baseline was obtained, pre-validated siRNA
177 (5 µg per side) against GluN2C or nonactive RNA sequence was injected bilaterally into VTA for two
178 consecutive days. Reward thresholds were measured 24-h after each injection. After 24 h, the last
179 threshold determination rats received a bilateral VTA microinjection of the NMDA antagonist, PPPA, and
180 reward thresholds were measured again immediately after injection for 120 min (see supplementary Fig.
181 S1 for experiment timeline).

182 **Western Blot**

183 Rats were decapitated immediately after the last behavioral test. Brains were removed and
184 directly placed on an ice-cold brain matrix and sectioned coronally. The VTA was dissected on an ice-
185 cooled plate from a 0.75-1mm slice using a 15-gauge tissue punch. The tissue was placed in a 1 ml
186 Eppendorf container and then immediately frozen at -80°C until biochemical experiments were
187 performed. VTA samples were mechanically homogenized in lysis buffer [10 mM Tris–HCl (pH 6.8), 2%
188 SDS and a cocktail protease inhibitor (Roche)]. The protein concentrations of the tissue samples were
189 measured using the BCA™ protein assay kit (Pierce, USA). Equal amounts of protein (10 µg) were
190 dissolved into 25 µl lysis buffer (which contained 4.5 µl 5X loading buffer and 0.5 µl β-mercaptoethanol),
191 boiled at 95°C for 5 min, and then subjected to SDS polyacrylamide gel electrophoresis (PAGE) with 8%
192 polyacrylamide and transferred to polyvinylidene difluoride (PVDF) membrane (BioRad Laboratories).
193 The membranes were blocked for 1 h in Tris buffered saline with Tween 20 (TBST) buffer with 5% bovine
194 serum albumin (BSA) and incubated with primary rabbit anti-β-actin antibody (Millipore Sigma, cat.
195 #SAB5600204) at 1:20000, with either primary mouse anti-GluN2C antibody (Novus Biological, cat. no.
196 #NBP2-29809) or mouse anti-GluN2A antibody (Millipore, cat. #SAB5200897) at 1:500 overnight at 4°C.
197 After rinsing 4 times with TBST for 5 min, the membranes were incubated with Horse Raddish
198 Peroxidase (HRP)-conjugated goat anti-mouse IgG secondary antibody (Cell Signaling, cat. #7076) at
199 1:20000 (to detect GluN2C or GluN2A) or HRP-conjugated goat anti-rabbit IgG secondary antibody (Cell
200 Signaling, cat. #7074) at 1:40000 (to detect β-actin) for 1 h. Membrane protein bands were detected
201 with ECL (BioRad) and visualized on the Chemidoc Biorad system (BioRad). Band densities were
202 measured and analyzed with Image Lab software (BioRad), and protein levels were normalized over β-
203 actin. The different subunits of the NMDAR were expressed as a percentage of control.

204 **Double-fluorescent in situ hybridization (FISH)**

205 Three naive Long-Evans male rats were anesthetized using an overdose of intraperitoneal ketamine
206 50 mg/kg, xylazine 5 mg/kg, and acepromazine 1 mg/kg perfused intracardially with ice-cold PBS. After
207 removal, the brains were rapidly frozen in dry ice-cooled 2-methyl butane (Fisher Scientific, Hampton,
208 NH, USA). Coronal sections of the VTA at 10 µm were obtained using a cryostat and mounted onto
209 superfrost slides (Fisher Scientific Ltd, Nepean, ON, Canada). Coronal cryosections were prepared, air
210 dried, fixed in 4% paraformaldehyde, and acetylated in 0.25% acetic anhydride/100 mM triethanolamine
211 (pH 8), followed by incubation for 30 minutes at room temperature in hybe solution. Then, slices were
212 incubated overnight at 60°C in 100 µl of hybe-solution buffer containing 20 ng digoxigenin (Dig)-labeled
213 probes (see below) for colorimetric detection (Roche, cat. #11277073910) or 20 µg of fluorescein-
214 labeled probes (see below) for fluorescent detection (Roche, cat. #11685619910). After hybridization,
215 sections were washed at 60°C with SSC buffers of decreasing strength (5X-0.2X), then washed at room
216 temperature with 0.2X SSC and maleic acid buffer containing tween 20 (MABT). After washing, sections
217 were blocked for 30 minutes with 20% FBS and 1% blocking solution. For colorimetric detection, Dig
218 epitopes were detected with alkaline phosphatase-coupled anti-Dig fab fragments antibody at 1:2500
219 (Millipore Sigma, cat. #11093274910), and the signal revealed with Nitro Blue Tetrazolium chloride/5-
220 Bromo-4-Chloro-3-Indolyl Phosphate, toluidine salt (NBT/BCIP) alkaline phosphatase chromogen
221 substrate solution (SigmaAldrich).

222 For fluorescent detection, sections were incubated with HRP-conjugated anti-fluorescein antibody
223 at 1:500 concentration. Signals were revealed with the Tyramide Signal Amplification (TSA plus biotin)
224 kit (PerkinElmer, cat. #NEL749A001KT) at 1:100 concentration, followed by incubation with neutravidin
225 Oregon Green conjugated at 1:500 (Invitrogen, cat. #A-6374). HRP activity was stopped by the
226 incubation of sections in 0.1 M glycine and 3% H_2O_2. Dig epitopes were detected with HRP-conjugated
227 anti-Dig antibody at 1:1000 (Roche cat. #11207733910) and revealed with the TSA kit (PerkinElmer, cat.

228 #NEL704A001KT) using Cy3 tyramide at 1:100. All sections were counterstained with DAPI and mounted
229 using Fluoromount (ThermoFisher Scientific, cat. #00-4958-02).

230

231 Double FISH was performed with RNA probes labeled with digoxigenin (Dig) for tyrosine
232 hydroxylase and RNA probes labeled with Fluorescein for Grin2C, consisting of a 678 bp fragment, (Fw
233 primer: 5'-ctactgctcccgtgaagagg-3', Rv primer: 5'-agagcttggtgtagggggtt-3'). The tyrosine hydroxylase
234 probe consisting of a fragment of 1142 bp was a kind gift from Prof. Marten Smidt (University of
235 Amsterdam). Cells were automatically counted using ImageJ FIJI software (NIH, USA). Briefly, each
236 channel was converted to binary and combined. This creates an image of only the cells that expressed
237 both TH and NR2C. Then we automatically counted the numbers of cells in the TH binary and the
238 number of cells in the TH+NR2C binary. The percentage was calculated by dividing the total number of
239 TH+ cells expressing NR2C by the total number of TH+ cells and multiplying the number by 100.

240

241 **qRT-PCR analysis**

242 Because no study has been carried out to determine the extent of the different NMDAR subunits
243 in the limbic brain regions involved in reward and motivation, we carried out the following quantitative
244 real-time RT-PCR study of the Grin2a-d transcript subtype. Brain punches from the prefrontal cortex
245 (PFC), nucleus accumbens (Nac), lateral hypothalamus (LH), habenula (Hab), amygdala (Amyg), bed
246 nucleus of the stria terminalis (BNst), ventral pallidum (VP), hippocampus (Hipp), pedunculopontine
247 tegmental nucleus (PPtg), ventral tegmental area (VTA), rostromedial tegmental nucleus (RMtg) and
248 raphe nucleus of four (n=4) naive Long-Evans male rats were taken. Total RNA was extracted using trizol
249 and purified on mini spin columns (RNeasy Kit protocol, Qiagen, Toronto, ON, Canada). All RNA samples
250 were determined to have values 260/280 and 260/230 values >1.8, using the Nanodrop 1000 system

251 (Thermo Scientific, Toronto, ON, Canada). We assessed the integrity of RNA by the presence of well-
252 defined 28S and 18S ribosomal bands and RNA integrity number ≥ 8 using the 2100 bioanalyzer
253 (Agilent). Reverse transcription (RT) for Grin2a, Grin2b, Grin2c, Grin2d, glyceraldehyde-3-
254 phosphatedehydrogenase (GAPDH), and hypoxanthine phosphoribosyltransferase (HPRT) was
255 performed (see primer sequences in supplementary Table 1). Real-time PCR, using a TaqMan assay, was
256 performed with an Applied Biosystems 7900HT RT PCR system on the Institute for Research on
257 Immunology and Cancer (IRIC) genomic platform (https://genomique.iric.ca/). Data were analyzed using
258 the relative quantification method (ΔΔ ct), and the levels of transcripts were normalized with both the
259 expression of the reference (housekeeping) genes, GAPDH and HPRT. We used two housekeeping genes
260 to make a robust determination of the levels of Grin2c across the brain areas studied. As expressed by
261 Vandesompele et al.(2002), the use of multiple housekeeping genes significantly decreases the
262 estimation error in qPCRs. When using multiple housekeeping genes for accurate normalization of the
263 relative gene expression, the geometric mean is used in the calculations.

264

265 **Data Analysis**

266 The fit of the rate frequency data and M50 value were obtained using MATLAB (Natick, MA).
267 Differences in M50 values and protein levels were assessed using the t-test. Data analysis was
268 performed using Statistica v12 (Tulsa, OK), and graphics were done in Origin v9 (Northamptom, MA).

269

270 **Results**

271 **Expression of NMDAR subunit mRNAs (Grin2a-d) in the VTA and other limbic areas**

272 Considering the role that glutamate and NMDAR play in modulating the limbic circuitry
273 implicated in motivation and, particularly, in relaying a reward signal in the VTA, we first investigated
274 the distribution of different NMDAR subunits throughout several limbic regions. We performed qRT-PCR
275 on mRNA taken from all relevant regions (Fig. 1: the prefrontal cortex (PFC), nucleus accumbens (Nac),
276 lateral hypothalamus (LH), habenula (Hab), amygdala (Amyg), bed nucleus of the stria terminalis (BNST),
277 ventral pallidum (VP), hippocampus (Hipp), pedunculopontine tegmental nucleus (PPtg), ventral
278 tegmental area (VTA), rostromedial tegmental nucleus (RMtg) and dorsal raphe nucleus (DR). As
279 expected, mRNA concentrations vary notably across brain areas, although in all areas examined, we
280 observed that the expression of the Grin2d subunit remained relatively low compared to other subunits.
281 In Hipp, the mRNA for the Grin2a and Grin2b subunits are the most abundant, followed by Grin2c.
282 Grin2b mRNA is the most abundant in the PFC, followed by Grin2a and Grin2c. Grin2b and Grin2c were
283 the most abundant in the nucleus accumbens, the ventral pallidum and the BNst. In Amyg Grin2b mRNA
284 was also the most abundant, but Grin2a was more elevated than Grin2c. A nearly similar content of
285 Grin2b and 2c was observed in LH and Hab. Grin2c was the most abundant in regions posterior to the
286 VTA, namely the PPTg, RMTg, and Raphe nuclei. We found that Grin2c mRNA is expressed within the
287 VTA, being as abundant as 2b. We also confirmed that the Grin2c transcript is translated into a protein
288 subunit (GluN2C) in the VTA (data not shown) by Western blotting.

289 To confirm and elaborate on the observation that VTA neurons express significant levels of
290 Grin2c, we performed an independent set of experiments to investigate the spatial expression of Grin2c
291 in the mesencephalon. The Allen Brain Atlas displays Grin2c expression in the mesencephalon, with
292 expression in the red nucleus (arrowhead, Fig. 2A) and SN and VTA region (arrow, Fig 2A) [34,35]. Using
293 the same probe, we confirmed the ample expression of Grin2c in the midbrain (Fig 2A). To verify if
294 Grin2c is expressed in DA neurons, we performed double-labeling fluorescent *in situ* hybridization and
295 observed co-expression of Th transcript and Grin2c in the VTA (Fig 2B). Quantitative analysis shows that

296 the level of colocalization of Grin2c and TH in DA neurons is around 46% (SEM= 7.83) (Fig. 2C and
297 supplementary Fig. S2). Together, these data suggest that Grin2c could be a relevant component in
298 transmitting glutamatergic signals by DA VTA neurons.

299 **Validation of siRNA effects on NMDA receptor subunit protein levels**

300 Knowing that the Grin2c is significantly expressed in VTA DA neurons, we set out to determine
301 its involvement in relaying the glutamate reward signal. To do so, we designed a strategy to specifically
302 down-regulate the NMDA receptor GluN2C protein subunit *in vivo* by injecting adult rats bilaterally with
303 siRNA against Grin2c transcript, or scrambled siRNA as a control, in the VTA (-5.5 AP, 3.2 ML at an angle
304 of 18 °, 6.5 DV from the skull surface). To confirm the efficacy and the specificity of the Grin2c siRNA, we
305 performed Western blots for GluN2C and GluN2A in total homogenates of VTA (immediately after the
306 last behavioral test). Microinjections of siRNA against Grin2c produced a significant 41% (SEM = 3.22)
307 decrease in the expression of the NMDAR receptor GluN2C subunit compared to the scrambled control
308 [$t_{(10)}$ =2.43; p=0.035] (Fig. 3A). Moreover, the active Grin2c siRNA was selective for GluN2C subunit since
309 we observed no change in protein expression of the GluN2A subunit [$t_{(10)}$ =0.28; p=0.783] (Fig. 3B).

310 **Down-regulation of the GluN2C subunit in VTA strongly reduces the Dorsal Raphe reward**
311 **signal.**

312 The selective downregulation of the NMDAR GluN2C subunit produced a decrease in reward-
313 seeking behavior. Figure 4 shows the behavioral data collected 24 h after the last siRNA microinjection
314 for representative subjects. Intra-VTA microinjections of the active siRNA against Grin2c produced a
315 rightward displacement of the curve that relates the nose-poke rate to the pulse frequency (R/F curve;
316 Fig. 4C), reflecting a reduction in transmission of the reward signal within the VTA. On the contrary, VTA
317 microinjections of the inactive RNA sequence did not affect the transmission of the reward signal as they
318 did not produce a significant displacement of the R/F curve (Fig. 4A).

319 To further characterize the specific role of the GluN2C subunit in relaying the reward signal in
320 VTA neurons, we used a pharmacological approach to the target NMDARs in animals that had received
321 either a scrambled or Grin2c siRNA injection. First, in animals microinjected with the inactive siRNA, the
322 NMDA antagonist, PPPA, enhanced the reward signal in the VTA; it produced a leftward displacement of
323 the R/F curve (Fig. 4B) so that lower frequencies delivery to the DR were required to generate a reward.
324 Interestingly, PPPA failed to alter the reward signal (no displacement of the R/F curve) in the animals
325 microinjected with the active Grin2c siRNA (Fig. 4D).

326 Figure 5 shows the average changes in the M50 reward index and the maximum response. Intra-
327 VTA injection of saline does not produce a significant change in the stimulation threshold (M50) [$t_{(19)}$ =
328 1.696; p=0.10] or the maximum response rate [$t_{(21)}$ = 1.009; p=0.3246] (Fig. 5 A-B). On the other hand,
329 intra-VTA injection of siRNA against Grin2c produced a 38.17% increase (SEM = 7.12) in M50 when
330 compared against their baseline, while the M50 of the rats that received the nonactive siRNA only
331 changed by 1.5 % (SEM = 2.95). The increase in M50 observed in the subjects that received the siRNA
332 against Grin2c is significantly different from that of the ones that received the scramble sequence (Fig.
333 5C) [$t_{(20)}$ =4.754 p=0.0001] and reflects a significant reduction in transmission of DR reward signal to VTA
334 neurons. Active siRNA also produced a small but significant 17.3% decrease in the maximum response
335 rate (Fig. 5D) [$t_{(21)}$ = 2.095; p=0.048].

336 The pharmacological manipulation of VTA glutamate using PPPA produced reliable changes in
337 M50 and maximum response rate only in the animals that received the inactive siRNA treatment. PPPA
338 enhanced the reward signal (reduction in M50 index, Fig. 5E). M50 decreased on average by 18.7 %
339 (SEM = 2.38), and the maximum response rate increased on average by 25% (SEM = 4.15; Fig. 5F). For
340 the subjects that received the siRNA against Grin2c, PPPA increased the M50 by 2% (SEM = 4.17) and the
341 maximum response rate by 3.6% (SEM=4.4) (Fig. 5E and 5F). The differences between the inactive and
342 active siRNA are significant for the changes produced in M50 for PPPA [$t_{(8)}$ =3.782 p=0.005] as well as for

343 the changes produced in the maximum rate PPPA [$t_{(8)}$ =3.534; p=0.007]. Together, these data suggest
344 that the GluN2C subunit is vital to relay the reward signal in VTA neurons.

345 **Discussion**

346 Glutamate-containing terminals establish synaptic contacts with VTA DA neurons [36,37] and
347 rewarding electrical stimulation is associated with an increase in VTA glutamate release [38]. Some of
348 those VTA terminals come from the DR, which sends the highest number and density of glutamatergic
349 projections [6].

350 Several studies have shown that NMDA receptors play a key role in activating DA neurons.
351 Iontophoretic administration of NMDA receptor antagonists [39], as well as genetic deletion of the
352 NMDA receptor GluN1 subunit from DA neurons, selectively attenuate DA phasic firing and reduces
353 learning in cue-dependent learning tasks [40]. VTA downregulation of the GluN1 subunit also decreases
354 brain stimulation reward [30]. Other research groups looking at depressive symptoms in rodents have
355 shown that inactivation of the GluN1 subunit in VTA altered VTA dopamine cells, which correlated with
356 behavioral deficits associated with anhedonia[41]. The fact that deletion or down-regulation of the
357 GluN1 subunit produces profound effects is not surprising, as this subunit is a necessary component in
358 forming functional NMDA receptor tetrameric complexes [42,43].

359 Here, we first measured Grin2 subunit transcript levels among several limbic brain regions
360 involved in motivated behaviors. The relative magnitude of each Grin2 mRNA level varied among
361 regions. Grin2a and Grin2b are the most abundant in the forebrain and diencephalic regions, while
362 Grin2d is the least abundant, findings that are consistent with previous reports (Ishii et al., 1993;
363 Monyer et al 1994). In more caudal mesencephalic regions such as VTA and DR, we found the Grin2c is
364 the most abundant, and the levels of Grin2d is much higher than in forebrain regions and the
365 hippocampus. These findings are also consistent we previous results (Fasulo and Hemby, 2003; Ishii et al

366 1993; Monyer et al., 1994). These results suggest an important and underappreciated role for the
367 NMDAR containing the GluN2C subunit in the limbic functions of these mesencephalic brain areas.

368 Another major finding of our study is that the NMDA receptor containing the GluN2C subunit
369 within the VTA is a necessary component for the transmission of the rewarding signal arising from DR.
370 Because the cellular machinery required for silencing the targeted RNA is primarily located in the
371 nucleus of a cell, VTA infusion of siRNA is expected to initially downregulate receptors expressed on cell
372 bodies located within the VTA, interfering with the mRNA and the processes required for protein
373 translation. Within the first 24h after the infusion, it must be less effective at reducing receptors located
374 on afferent terminals. Our selective GluN2C subunit downregulation *via* siRNA produced a significant
375 reduction in brain stimulation reward and a change in the performance capacity; effects were detected
376 24h after the first infusion. These reductions are inferred by the rightward and downward (reduction in
377 asymptote) displacement of the R/F curve [44]. Both effects could be associated with a reduction in the
378 release of DA from the nucleus accumbens since this decrease can affect both reward and motor
379 function [45]. It has been shown that electrical and optical stimulation of DR neurons produces an
380 increase in DA cell firing and DA phasic release [2,15,46] via glutamatergic DR efferents to the VTA
381 [1,2,20]. Substantial reduction in the GluN2C input likely decreases glutamatergic excitability in DA
382 neurons, reducing the overall DA release in terminal areas. The reduction of brain stimulation reward is
383 specific to GluN2C since a previous study showed that downregulation of GluN2A or/and GluN2D did not
384 produce a significant change in the curve that relates stimulation of the DR with nose-poke behavior
385 [30].

386 Our double fluorescent hybridization data show that a substantial amount of Grin2c mRNA is
387 colocalized in VTA TH+ cells. This observation is in line with single-cell expression profiling on DA
388 neurons, which shows that the Grin2c mRNA is expressed in mesocorticolimbic DA neurons [47–49].
389 Using qRT-PCR, we observed that Grin2c mRNA is the most abundantly expressed in DR and VTA

390 compared to other Grin2 subunit transcripts. In fact, Grin2c mRNA is expressed in all areas of the brain
391 observed in the adult rat brain, but its relative expression changes accordingly to where it is measured in
392 the anterior-posterior axis. In comparison, the Grin2a and Grin2b transcripts are the most abundant
393 mRNAs in the anterior and medial parts of the brain, the balance shifts towards Grin2c in posterior brain
394 areas. This observation is significant because, until recently, not many studies have been done regarding
395 the role of this NMDA receptor subunit, which was believed to be confined to the cerebellum, thalamus,
396 and olfactory bulb and to be present at very low levels in the hippocampus of the adult rodent brain
397 [50,51]. However, present results and recent observations using novel reporter mice [52] suggest this is
398 not the case.

399 Moreover, there is accumulating evidence that the NMDA receptor containing the GluN2C
400 subunit plays an important role in several domains. For example, NMDA receptors containing GluN2C
401 are required for the acquisition of conditioned fear and working memory because Grin2c knockout mice
402 show deficits in associating cues with aversive consequences, as well as navigating an eight-arm radial
403 maze [53]. Also, they spend more time immobile in the forced swim test [54]. At the cortical level, this
404 receptor controls the balance of excitatory and inhibitory activity in the medial prefrontal cortex since
405 Grin2c knockout mice have reduced excitatory postsynaptic currents, increased inhibitory postsynaptic
406 currents, and reduced spine density [55].

407 Can a downregulation of Grin2c mRNA in VTA TH- cells contribute to the reduction in reward
408 observed in this study? It is well known that VTA interneurons provide a strong, tonic, inhibitory drive
409 onto DA neurons. A reduction in glutamate excitatory input to these inhibitory neurons allows DA cells
410 to go from a silent state into a tonic firing state, increasing the likelihood that they will fire in phasic
411 mode. Such a change in DA firing mode is expected to translate into an enhancement of reward rather
412 than the attenuation we observed. Therefore, it is unlikely that GluN2C-containing NMDA receptors
413 containing GluN2C in these TH- cells play a role in relaying the reward signal.

414 To further characterize the effect of down-regulation of the GluN2C receptor in TH+ cells, we
415 injected PPPA, an NMDA receptor antagonist, into the VTA. Previous studies from our laboratory
416 [5,30,32] have shown that PPPA enhances brain stimulation reward, an effect that could be explained by
417 a reduction in the excitatory drive to VTA inhibitory interneurons. Consistent with our previous results,
418 PPPA produced a reliable enhancement in reward and performance; however, these effects were only
419 observed in the animals that received the inactive siRNA; in those animals where the GluN2C subunit
420 was downregulated, PPPA produced no change in brain stimulation reward. These results suggest that
421 Glun2C subunit are also involved in the excitatory drive to VTA inhibitory interneurons; the reduction in
422 the reward that we observed following local infusion of Grin2c siRNA must result from the net effect of
423 disinhibition and excitation of VTA DA signaling; therefore, unable to substantially change brain
424 stimulation reward.

425 **Technical Considerations**

426 It has been demonstrated that the detection of specific reward changes in the presence of a decrease in
427 operant response cannot be achieved by the unique measure of the response rate. To circumvent this
428 problem, we applied the psychophysical technique (curve shift method), a technique that allows us to
429 determine a reliable index of brain stimulation reward (M50) when used with the appropriate
430 parameters (0.1 ms cathodal pulses, fixed train duration, and fixed current intensity) of electrical
431 stimulation (Gallistel et al., 1980). The M50 index is indeed sensitive to changes in rates of responding,
432 but as shown by Miliaressis et al (1985) and Fouriezos et al (1990), the mean 50% increase in M50 that
433 we measured after injection of the active siRNA cannot be due to the mean 15% decrease in maximum
434 rates of responding that we also observed; it can only be the consequence of a specific reward
435 attenuation. Although electrical stimulation does not allow activating a selective population of neurons,
436 it is used here with a psychophysical method that permits us to detect attenuation of brain stimulation
437 reward that results from a reduction in VTA GluN2C subunits.

438 **Conclusion**

439 We demonstrated that a localized decrease in GluN2C-containing NMDA receptors in the VTA
440 significantly alters the rewarding signal originated in the DR. This observation adds to other studies
441 suggesting that the GluN2C receptor plays an important role in several disorders, including drug abuse
442 [56] and schizophrenia [53,55]. Furthermore, our results suggest that the levels of this receptor in the
443 VTA might be at the root of anhedonia.

444

445 **References**

446 [1] Mcdevitt RA, Tiran-cappello A, Harvey BK, Bonci A, Shen H, Balderas I, et al. Serotonergic versus
447 Nonserotonergic Dorsal Raphe Projection Neurons: Differential Participation in Reward Article
448 Serotonergic versus Nonserotonergic Dorsal Raphe Projection Neurons: Differential
449 Participation in Reward Circuitry 2014:1857–69.

450 [2] Qi J, Zhang S, Wang H-L, Wang H, de Jesus Aceves Buendia J, Hoffman AF, et al. A glutamatergic
451 reward input from the dorsal raphe to ventral tegmental area dopamine neurons. Nat Commun
452 2014;5:5390. https://doi.org/10.1038/ncomms6390.

453 [3] Boye SM, Rompré P-P. Mesencephalic substrate of reward: Axonal connections. J Neurosci
454 1996;16:3511–20.

455 [4] Hernandez G, Khodami-Pour A, Lévesque D, Rompré PP. Reduction in ventral midbrain NMDA
456 receptors reveals two opposite modulatory roles for glutamate on reward.
457 Neuropsychopharmacology 2015;40:1682–91. https://doi.org/10.1038/npp.2015.14.

458 [5] Bergeron S, Rompré P-P. Blockade of ventral midbrain NMDA receptors enhances brain

459 stimulation reward: a preferential role for GluN2A subunits. Eur Neuropsychopharmacol
460 2013;23:1623–35. https://doi.org/10.1016/j.euroneuro.2012.12.005.

461 [6] Watabe-Uchida M, Zhu L, Ogawa SK, Vamanrao A, Uchida N. Whole-brain mapping of direct
462 inputs to midbrain dopamine neurons. Neuron 2012;74:858–73.
463 https://doi.org/10.1016/j.neuron.2012.03.017.

464 [7] Wise R a. Dopamine, learning and motivation. Nat Rev Neurosci 2004;5:483–94.
465 https://doi.org/10.1038/nrn1406.

466 [8] Hernandez G, Breton Y-A, Conover K, Shizgal P. At what stage of neural processing does cocaine
467 act to boost pursuit of rewards? PLoS One 2010;5:e15081.
468 https://doi.org/10.1371/journal.pone.0015081.

469 [9] Hernandez G, Trujillo-Pisanty I, Cossette M-P, Conover K, Shizgal P. Role of Dopamine Tone in the
470 Pursuit of Brain Stimulation Reward. J Neurosci 2012;32:11032–41.
471 https://doi.org/10.1523/JNEUROSCI.1051-12.2012.

472 [10] Schultz W. A Neural Substrate of Prediction and Reward. Science (80-) 1997;275:1593–9.
473 https://doi.org/10.1126/science.275.5306.1593.

474 [11] Salamone JD. Behavioral pharmacology of dopamine systems: A new synthesis. mesolimbic
475 dopamine Syst. From Motiv. to action, 1991, p. 599–614.

476 [12] Wise R a, Rompre PP. Brain dopamine and reward. Annu Rev Psychol 1989;40:191–225.
477 https://doi.org/10.1146/annurev.ps.40.020189.001203.

478 [13] Simon H, Le Moal M, Cardo B. Intracranial self-stimulation from the dorsal raphe nucleus of the
479 rat: effects of the injection of para-chlorophenylalanine and of alpha-methylparatyrosine. Behav

480 Biol 1976. https://doi.org/10.1016/S0091-6773(76)91486-3.

481 [14] Rompre PP, Miliaressis E. Pontine and mesencephalic substrates of self-stimulation. Brain Res
482 1985;359:246–59.

483 [15] Moisan J, Rompre PP. Electrophysiological evidence that a subset of midbrain dopamine neurons
484 integrate the reward signal induced by electrical stimulation of the posterior mesencephalon.
485 Brain Res 1998;786:143–52. https://doi.org/doi:10.1016/S0006-8993(97)01457-1.

486 [16] Jacobs BL, Azmitia EC. Structure and function of the brain serotonin system. Physiol Rev
487 1992;72:165–230. https://doi.org/10.1152/physrev.1992.72.1.165.

488 [17] Vasudeva RK, Lin RCS, Simpson KL, Waterhouse BD. Functional organization of the dorsal raphe
489 efferent system with special consideration of nitrergic cell groups. J Chem Neuroanat
490 2011;41:281–93. https://doi.org/10.1016/j.jchemneu.2011.05.008.

491 [18] Wang RY, Aghajani GK. Antidromically identified serotonergic neurons in the rat midbrain raphe:
492 evidence for collateral inhibition. Brain Res 1977. https://doi.org/10.1016/0006-8993(77)90719-
493 3.

494 [19] Rompré PP, Miliaressis E. Behavioral determination of refractory periods of the brainstem
495 substrates of self-stimulation. Behav Brain Res 1987;23:205–19.

496 [20] Liu Z, Zhou J, Li Y, Hu F, Lu Y, Ma M, et al. Dorsal Raphe Neurons Signal Reward through 5-HT and
497 Glutamate. Neuron 2014;81:1360–74. https://doi.org/10.1016/j.neuron.2014.02.010.

498 [21] Sesack SR, Carr DB, Omelchenko N, Pinto A. Anatomical Substrates for Glutamate-Dopamine
499 Interactions. Ann N Y Acad Sci 2003;1003:36–52. https://doi.org/10.1196/annals.1300.066.

500 [22] Mogenson GJ, Jones DL, Yim CY. From motivation to action: functional interface between the

501 limbic system and the motor system. Prog Neurobiol 1980;14:69–97.
502 https://doi.org/10.1016/0301-0082(80)90018-0.

503 [23] Chergui K, Charléty PJ, Akaoka H, Saunier CF, Brunet J -L, Buda M, et al. Tonic Activation of NMDA
504 Receptors Causes Spontaneous Burst Discharge of Rat Midbrain Dopamine Neurons In Vivo. Eur J
505 Neurosci 1993;5:137–44. https://doi.org/10.1111/j.1460-9568.1993.tb00479.x.

506 [24] Grace AA, Bunney BS. The control of firing pattern in nigral dopamine neurons: burst firing. J
507 Neurosci 1984;4:2877–90. https://doi.org/6150071.

508 [25] Hyland BI, Reynolds JNJ, Hay J, Perk CG, Miller R. Firing modes of midbrain dopamine cells in the
509 freely moving rat. Neuroscience 2002;114:475–92. https://doi.org/10.1016/S0306-
510 4522(02)00267-1.

511 [26] Suaud-Chagny MF, Chergui K, Chouvet G, Gonon F. Relationship between dopamine release in
512 the rat nucleus accumbens and the discharge activity of dopaminergic neurons during local in
513 vivo application of amino acids in the ventral tegmental area. Neuroscience 1992.
514 https://doi.org/10.1016/0306-4522(92)90076-E.

515 [27] Tsai H-C, Zhang F, Adamantidis A, Stuber GD, Bonci A, de Lecea L, et al. Phasic firing in
516 dopaminergic neurons is sufficient for behavioral conditioning. Science 2009;324:1080–4.
517 https://doi.org/10.1126/science.1168878.

518 [28] Pérez-Otaño I, Schulteis CT, Contractor A, Lipton SA, Trimmer JS, Sucher NJ, et al. Assembly with
519 the NR1 subunit is required for surface expression of NR3A-containing NMDA receptors. J
520 Neurosci 2001;21:1228–37. https://doi.org/10.1523/jneurosci.21-04-01228.2001.

521 [29] McIlhinney RAJ, Le Bourdellès B, Molnár E, Tricaud N, Streit P, Whiting PJ. Assembly intracellular
522 targeting and cell surface expression of the human N-methyl-D-aspartate receptor subunits NR1a

523 and NR2A in transfected cells. Neuropharmacology 1998;37:1355–67.
524 https://doi.org/10.1016/S0028-3908(98)00121-X.

525 [30] Hernandez G, Khodami-Pour A, Lévesque D, Rompré P-PP. Reduction in Ventral Midbrain NMDA
526 Receptors Reveals Two Opposite Modulatory Roles for Glutamate on Reward.
527 Neuropsychopharmacology 2015;40:1682–91. https://doi.org/10.1038/npp.2015.14.

528 [31] Salahpour A, Medvedev IO, Beaulieu J-M, Gainetdinov RR, Caron MG. Local knockdown of genes
529 in the brain using small interfering RNA: a phenotypic comparison with knockout animals. Biol
530 Psychiatry 2007;61:65–9. https://doi.org/10.1016/j.biopsych.2006.03.020.

531 [32] Ducrot C, Fortier E, Bouchard C, Rompré P-P. Opposite modulation of brain stimulation reward by
532 NMDA and AMPA receptors in the ventral tegmental area. Front Syst Neurosci 2013;7:57.
533 https://doi.org/10.3389/fnsys.2013.00057.

534 [33] Vandesompele J, De Preter K, Pattyn F, Poppe B, Van Roy N, De Paepe A, et al. Accurate
535 normalization of real-time quantitative RT-PCR data by geometric averaging of multiple internal
536 control genes. Genome Biol 2002;3:RESEARCH0034. https://doi.org/10.1186/gb-2002-3-7-
537 research0034.

538 [34] Lein ES, Hawrylycz MJ, Ao N, Ayres M, Bensinger A, Bernard A, et al. Genome-wide atlas of gene
539 expression in the adult mouse brain. Nature 2007;445:168–76.
540 https://doi.org/10.1038/nature05453.

541 [35] Allen Institute for Brain Science. Allen Mouse Brain Atlas 2010. https://mouse.brain-
542 map.org/search/index.

543 [36] Carr DB, Sesack SR. Projections from the rat prefrontal cortex to the ventral tegmental area:
544 target specificity in the synaptic associations with mesoaccumbens and mesocortical neurons. J

545 Neurosci 2000;20:3864–73.

546 [37] Omelchenko N, Sesack SR. Ultrastructural analysis of local collaterals of rat ventral tegmental
547 area neurons: GABA phenotype and synapses onto dopamine and GABA cells. Synapse
548 2009;63:895–906. https://doi.org/10.1002/syn.20668.

549 [38] You ZB, Chen YQ, Wise RA. Dopamine and glutamate release in the nucleus accumbens and
550 ventral tegmental area of rat following lateral hypothalamic self-stimulation. Neuroscience
551 2001;107:629–39. https://doi.org/10.1016/S0306-4522(01)00379-7.

552 [39] Overton P, Clark D. Iontophoretically administered drugs acting at the N-methyl-D-aspartate
553 receptor modulate burst firing in A9 dopamine neurons in the rat. Synapse 1992;10:131–40.
554 https://doi.org/10.1002/syn.890100208.

555 [40] Zweifel LS, Parker JG, Lobb CJ, Rainwater A, Wall VZ, Fadok JP, et al. Disruption of NMDAR-
556 dependent burst firing by dopamine neurons provides selective assessment of phasic dopamine-
557 dependent behavior. Proc Natl Acad Sci 2009;106:7281–8.
558 https://doi.org/10.1073/pnas.0813415106.

559 [41] Jastrzebska K, Walczak M, Cieslak PE, Szumiec L, Turbasa M, Engblom D, et al. Loss of NMDA
560 receptors in dopamine neurons leads to the development of affective disorder-like symptoms in
561 mice. Sci Rep 2016;6:1–11. https://doi.org/10.1038/srep37171.

562 [42] Monyer H, Sprengel R, Schoepfer R, Herb A, Higuchi M, Lomeli H, et al. Heteromeric NMDA
563 Receptors: Molecular and Functional Distinction of Subtypes. Science (80-) 1992;256:1217–21.
564 https://doi.org/10.1126/science.256.5060.1217.

565 [43] Nakanishi S. Molecular diversity of glutamate receptors and implications for brain function.
566 Science (80-) 1992;258:597–603. https://doi.org/10.1126/science.1329206.

567 [44] Miliaressis E, Rompre PP, Laviolette P, Philippe L, Coulombe D. The curve-shift paradigm in self-
568 stimulation. Physiol Behav 1986;37:85–91. https://doi.org/10.1016/0031-9384(86)90388-4.

569 [45] Stellar JR, Kelley a E, Corbett D. Effects of peripheral and central dopamine blockade on lateral
570 hypothalamic self-stimulation: evidence for both reward and motor deficits. Pharmacol Biochem
571 Behav 1983;18:433–42.

572 [46] Hernandez G, Cossette MP, Shizgal P, Rompré PP. Ventral midbrain NMDA receptor blockade:
573 From enhanced reward and dopamine inactivation. Front Behav Neurosci 2016;10:1–11.
574 https://doi.org/10.3389/fnbeh.2016.00161.

575 [47] Anderegg A, Poulin JF, Awatramani R. Molecular heterogeneity of midbrain dopaminergic
576 neurons - Moving toward single cell resolution. FEBS Lett 2015;589:3714–26.
577 https://doi.org/10.1016/j.febslet.2015.10.022.

578 [48] Saunders A, Macosko EZ, Wysoker A, Goldman M, Krienen FM, de Rivera H, et al. Molecular
579 Diversity and Specializations among the Cells of the Adult Mouse Brain. Cell 2018;174:1015-
580 1030.e16. https://doi.org/10.1016/j.cell.2018.07.028.

581 [49] Poulin JF, Gaertner Z, Moreno-Ramos OA, Awatramani R. Classification of Midbrain Dopamine
582 Neurons Using Single-Cell Gene Expression Profiling Approaches. Trends Neurosci 2020;43:155–
583 69. https://doi.org/10.1016/j.tins.2020.01.004.

584 [50] Monyer H, Burnashev N, Laurie DJ, Sakmann B, Seeburg PH. Developmental and regional
585 expression in the rat brain and functional properties of four NMDA receptors. Neuron
586 1994;12:529–40. https://doi.org/10.1016/0896-6273(94)90210-0.

587 [51] Wenzel A, Scheurer L, Künzi R, Fritschy JM, Mohler H, Benke D. Distribution of NMDA receptor
588 subunit proteins NR2A, 2B, 2C and 2D in rat brain. Neuroreport 1995;7:45–8.

589 [52] Ravikrishnan A, Gandhi PJ, Shelkar GP, Liu J, Pavuluri R, Dravid SM. Region-specific Expression of
590 NMDA Receptor GluN2C Subunit in Parvalbumin-Positive Neurons and Astrocytes: Analysis of
591 GluN2C Expression using a Novel Reporter Model. Neuroscience 2018;380:49–62.
592 https://doi.org/10.1016/j.neuroscience.2018.03.011.

593 [53] Hillman BG, Gupta SC, Stairs DJ, Buonanno A, Dravid SM. Behavioral analysis of NR2C knockout
594 mouse reveals deficit in acquisition of conditioned fear and working memory. Neurobiol Learn
595 Mem 2011;95:404–14. https://doi.org/10.1016/j.nlm.2011.01.008.

596 [54] Shelkar GP, Pavuluri R, Gandhi PJ, Ravikrishnan A, Gawande DY, Liu J, et al. Differential effect of
597 NMDA receptor GluN2C and GluN2D subunit ablation on behavior and channel blocker-induced
598 schizophrenia phenotypes. Sci Rep 2019;9:1–11. https://doi.org/10.1038/s41598-019-43957-2.

599 [55] Gupta SC, Ravikrishnan A, Liu J, Mao Z, Pavuluri R, Hillman BG, et al. The NMDA receptor GluN2C
600 subunit controls cortical excitatory-inhibitory balance, neuronal oscillations and cognitive
601 function. Sci Rep 2016;6:1–13. https://doi.org/10.1038/srep38321.

602 [56] Joffe ME, Grueter BA. Cocaine Experience Enhances Thalamo-Accumbens N-Methyl-D-Aspartate
603 Receptor Function. Biol Psychiatry 2016;80:671–81.
604 https://doi.org/10.1016/j.biopsych.2016.04.002.

605

606

607 **Figure Captions**

608 **Figure 1. Relative expression of NMDAR containing Grin2a-d subunits mRNA across different brain**
609 **areas.** Brain punches from the prefrontal cortex (PFC), nucleus accumbens (Nac), lateral hypothalamus
610 (LH), habenula (Hab), amygdala (Amyg), bed nucleus of the stria terminalis (BNST), ventral pallidum (VP),
611 hippocampus (Hipp), pedunculopontine tegmental nucleus (PPtg), ventral tegmental area (VTA),
612 rostromedial tegmental nucleus (RMtg) and raphe nucleus (Raphe were analyzed) (n=4). Relative mRNA
613 levels were quantified using $\Delta\Delta$ ct method. Histogram bars represent relative mRNA levels normalized
614 over both GAPDH and HPRT mRNA levels.

615 **Figure 2. Double FISH immunodetection shows a high colocalization of Grin2c in TH positive cells of**
616 **the VTA. A.** Representative images of the ventral midbrain area containing the SN and VTA taken from
617 the Allen Brain Atlas, displaying Grin2c transcript in the red nucleus (arrowhead) and SN and VTA area
618 (arrow). B-B". Fluorescent *in situ* hybridization reveals that Grin2c expression (Fluorescein; green)
619 overlaps with tyrosine hydroxylase (TH) (Cy3; red) in the mesencephalon, scale represents 50 µm. **C.** Bar
620 graphs showing the count of TH and Grin2c positive cells in the VTA.

621 **Figure 3. Grin2c intra-VTA siRNA injections significantly reduce GluN2C subunit protein levels in the**
622 **VTA. A)** siRNA microinjections against Grin2c subunit transcript produces a significant reduction in this
623 subunit immunoreactivity. The histogram bars represent means +/- SEM of normalized NMDAR GluN2C
624 subunit protein levels in animals injected with the Grin2c siRNA or the negative control siRNA (N=12 per
625 condition) (*$p < 0.05$; Student's t-test) in VTA homogenates. The inset shows representative examples of
626 signals from GluN2C and β-actin after Western blotting procedure. **B)** The histogram bars represent
627 means +/- SEM of normalized NMDAR GluN2A subunit protein levels in animals injected with the Grin2c
628 siRNA or the negative control siRNA (N=12 per condition) in VTA homogenates. The inset shows
629 representative examples of signals from GluN2A and β-actin after Western blotting procedure.

630 **Figure 4. Intra-VTA Grin2c siRNA injection reduced rate-frequency response from dorsal raphe**
631 **stimulation.** The figure shows representative rate-frequency curves for selected subjects showing the
632 effect of the different siRNA treatment and intra-VTA injection of PPPA (0.825 nmol/0.5µl/side). **A)**
633 Treatment with the negative control siRNA (0.5 µg/side) produced no effect on the curve that relates
634 the nose-poke rate with the electrical pulse trains. The baseline curve and the one obtained 24-h after
635 the first and second siRNA injections overlap. **B)** In the animals treated with the negative control siRNA
636 Intra-VTA injection with PPPA produced a leftward and upward shift of rate-frequency curve. **C)**
637 Treatment with siRNA (0.5µg /side) against Grin2c produced a decrease of the rewarding effects that
638 arise from dorsal raphe electrical stimulation. When contrasted against the baseline curves, the rate
639 frequency curve obtained 24-h after the last siRNA injection is displaced to the right. A decrease in the
640 upper asymptote is also observed. Interestingly, the Grin2c siRNA treatment alters PPPA effect. **D)** siRNA
641 injections against Grin2c obliterate the effects of PPPA on brain stimulation reward and motor
642 performance. The pretreatment with the Grin2c siRNA renders PPPA ineffective for modifying the
643 reward signal that arises from dorsal raphe stimulation.

644 **Figure 5. Shifts caused by control and Grin2c siRNAs in stimulation threshold and maximum response**
645 **rate. A-B)** Histogram bars represent means +/- SEM; saline injection in the VTA does not produces a
646 reliable change in M50 nor MAX **C)** Treatment with the control siRNA did not produce a significant
647 change in the stimulation threshold (M50), but the treatment with the siRNA against the Grin2c subunit
648 produces a significant increase. **D)** The siRNA against Grin2c produced a significant decrease in the
649 maximum response rate (MAX) compared to subjects that received the scramble siRNA. **E)** siRNA
650 downregulation of the Grin2c subunit in the VTA abolishes the enhancing effect of PPPA. PPPA produced
651 a decrease in the self-stimulation threshold only in those animals that were pre-treated with the
652 scrambled siRNA. The self-stimulation threshold showed no reliable change in those animals pre-treated
653 with the siRNA against Grin2c. The PPPA enhancement effect on M50 values in the scrambled siRNA

654 group is significantly different from that of the group that received the siRNA against Grin2c. **F)** Similarly,
655 PPPA only produced an increase in the maximum response rate in those animals that were pre-treated
656 with the scrambled siRNA and not with the siRNA against Grin2C. The gray area denotes the 95%
657 confidence interval of the baseline curves. (*p <0.05, ** p<0.01, *** p<0.0001; Student's t-test).

658

659 **Supplementary Figure 1: Schematic of the experimental behavioral procedure.**

660 **Supplementary Figure 2: Low-level magnification of Double FISH immunodetection.**

661 **Supplementary Table 1: Primer sequences for qRT-PCR Grin2a-d analysis**

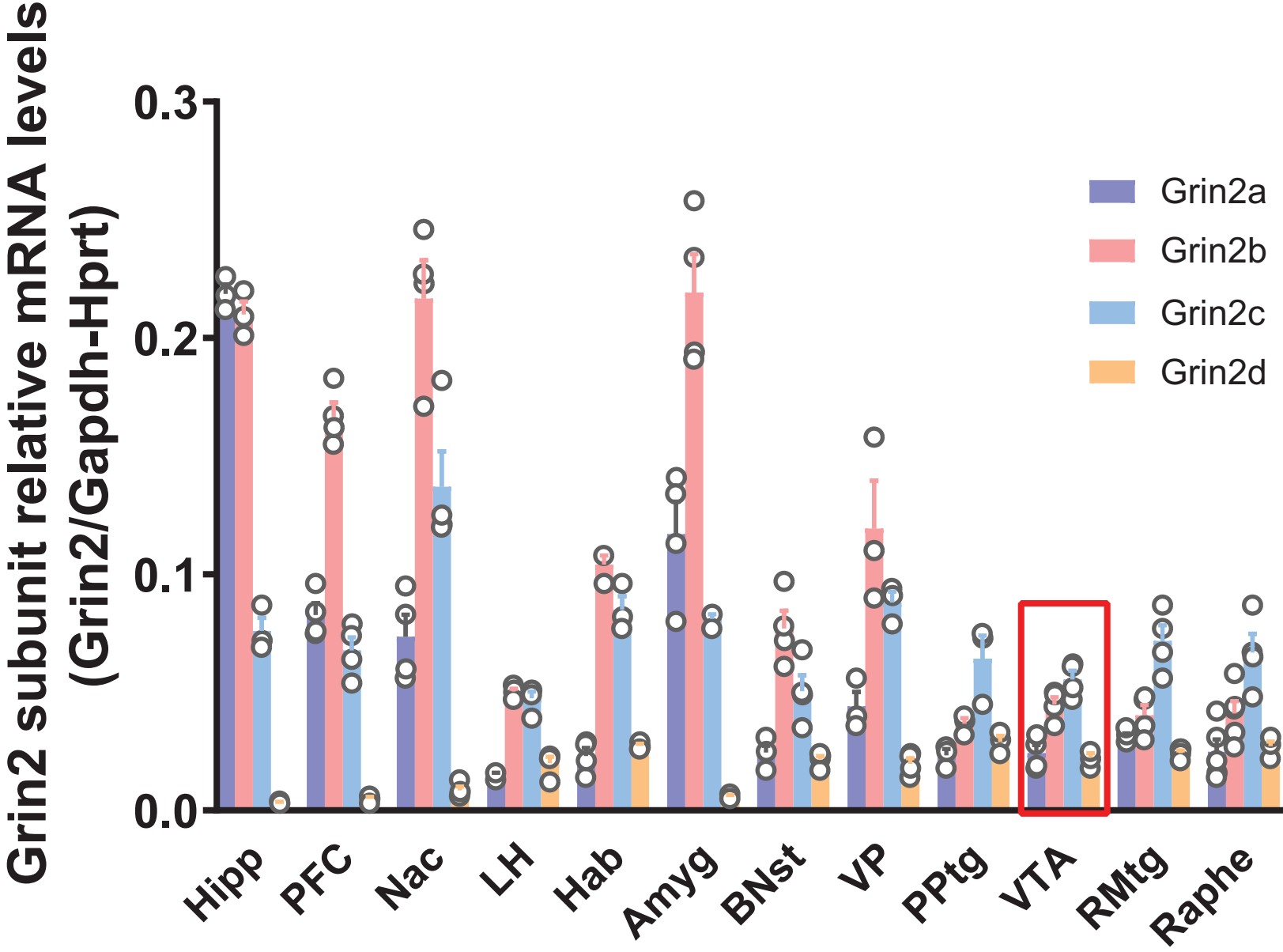
Grin2 subunit relative mRNA levels
(Grin2/Gapdh-Hprt)
0.3
0.2
0.1
0.0
Grin2a
Grin2b
Grin2c
Grin2d
Hipp
PFC
Nac
LH
Hab
Amyg
BNst
VP
PPtg
VTA
RMtg
Raphe

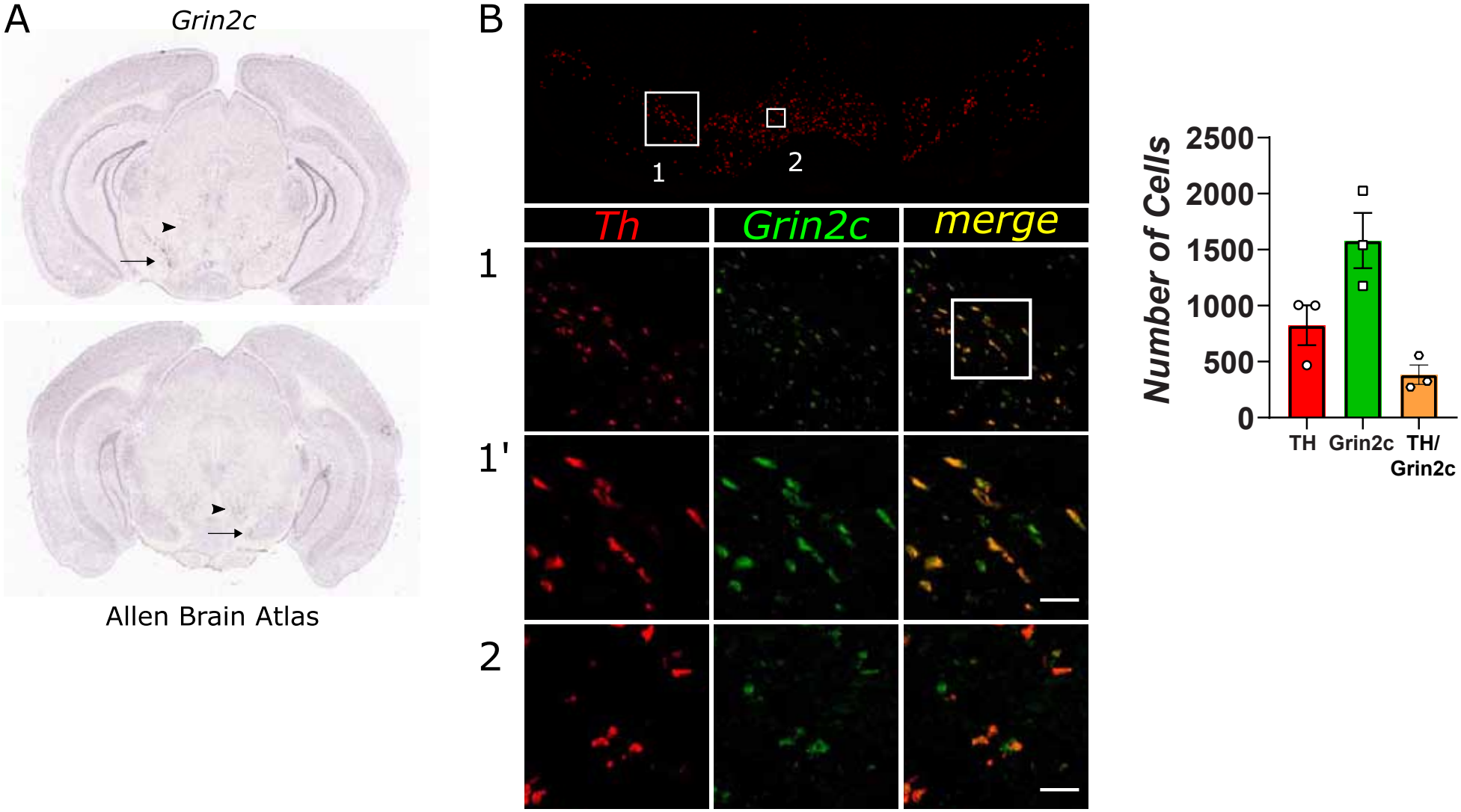
A
Grin2c
Allen Brain Atlas
B
1
2
Th
Grin2c
merge
1
1'
2
Number of Cells
2500
2000
1500
1000
500
0
TH
Grin2c
TH/
Grin2c

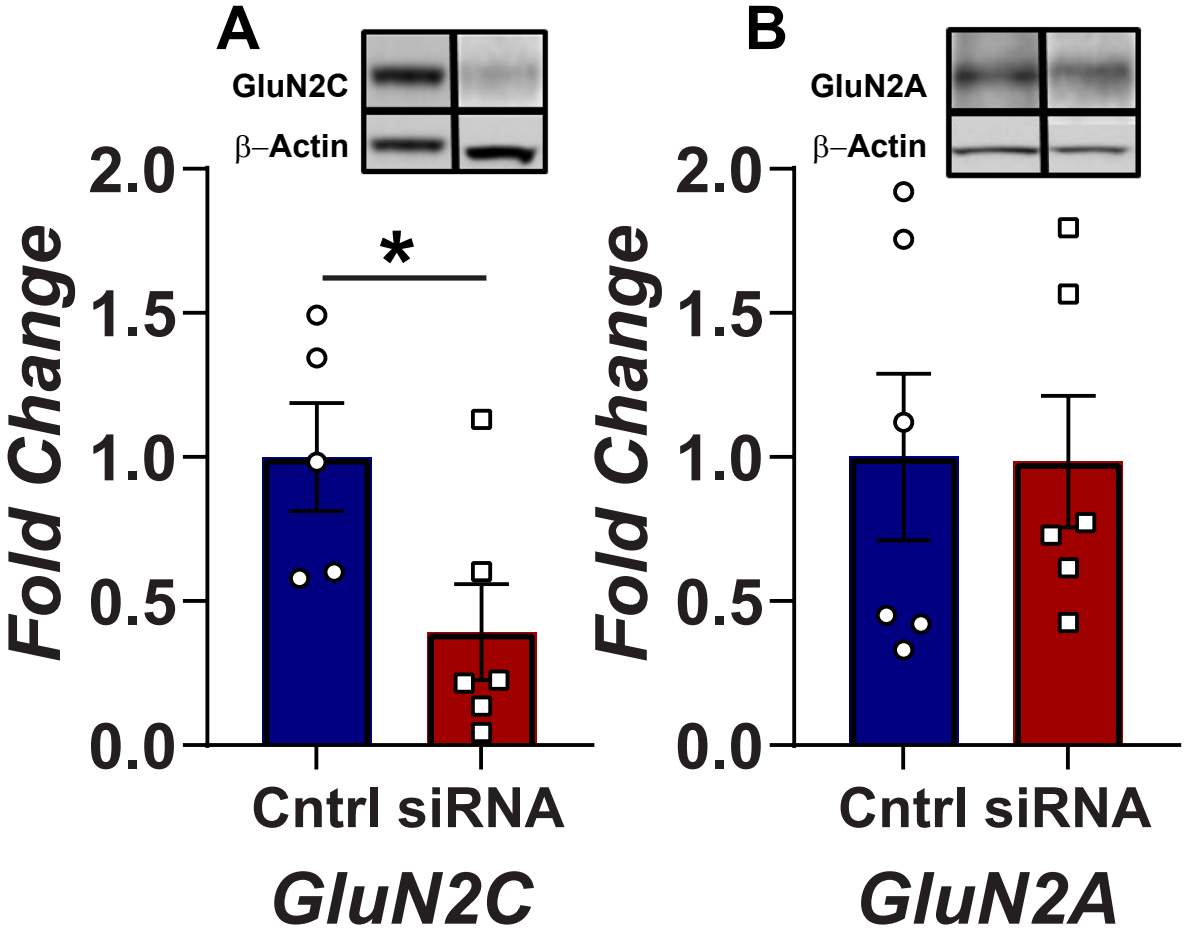
A
GluN2C
β–Actin
2.0
1.5
1.0
0.5
0.0
Fold Change
*
Cntrl siRNA
GluN2C
B
GluN2A
β–Actin
2.0
1.5
1.0
0.5
0.0
Fold Change
Cntrl siRNA
GluN2A

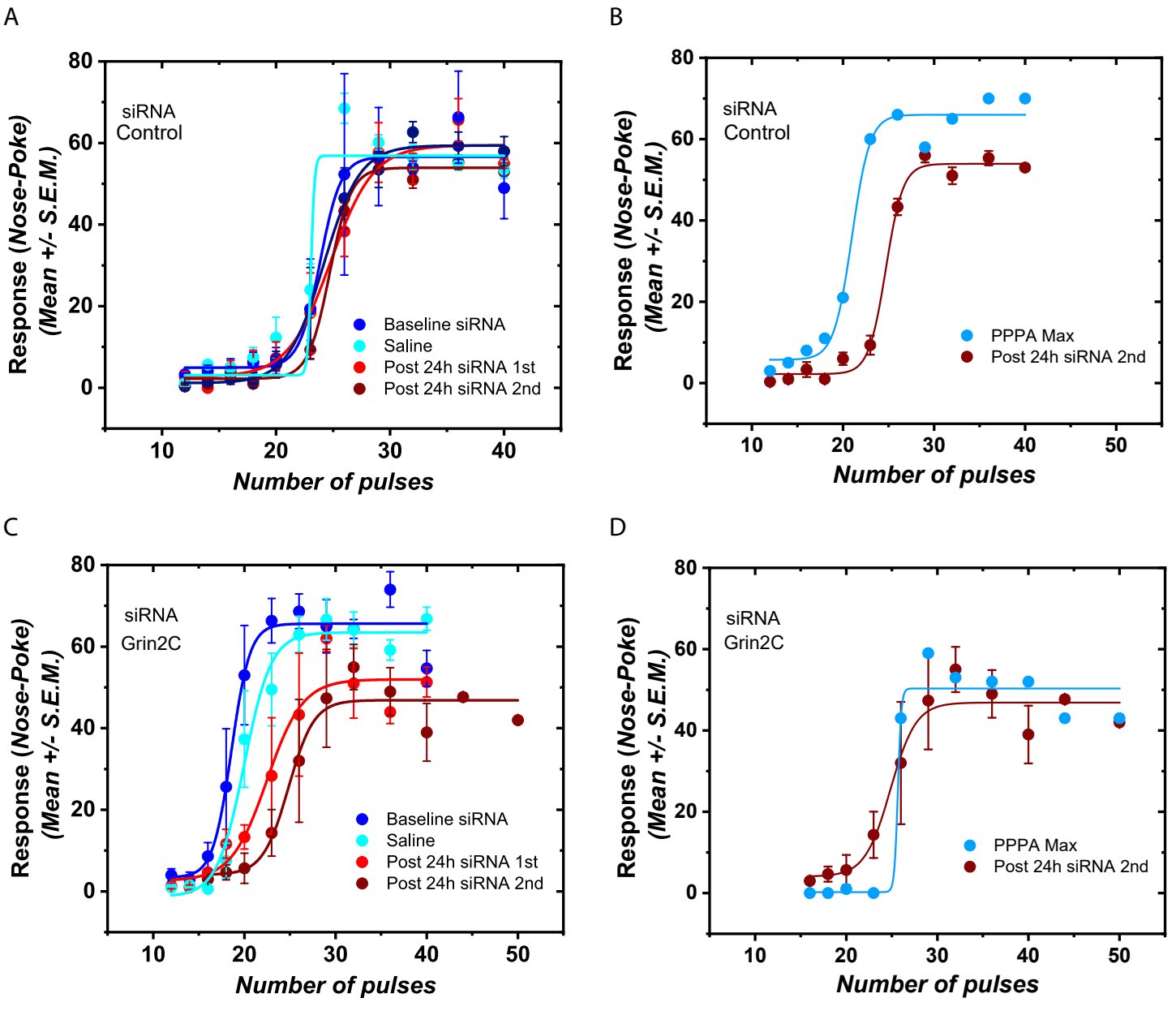
A
siRNA
Control
Baseline siRNA
Saline
Post 24h siRNA 1st
Post 24h siRNA 2nd
Response (Nose-Poke)
(Mean +/- S.E.M.)
Number of pulses
B
siRNA
Control
PPPA Max
Post 24h siRNA 2nd
Response (Nose-Poke)
(Mean +/- S.E.M.)
Number of pulses
C
siRNA
Grin2C
Baseline siRNA
Saline
Post 24h siRNA 1st
Post 24h siRNA 2nd
Response (Nose-Poke)
(Mean +/- S.E.M.)
Number of pulses
D
siRNA
Grin2C
PPPA Max
Post 24h siRNA 2nd
Response (Nose-Poke)
(Mean +/- S.E.M.)
Number of pulses

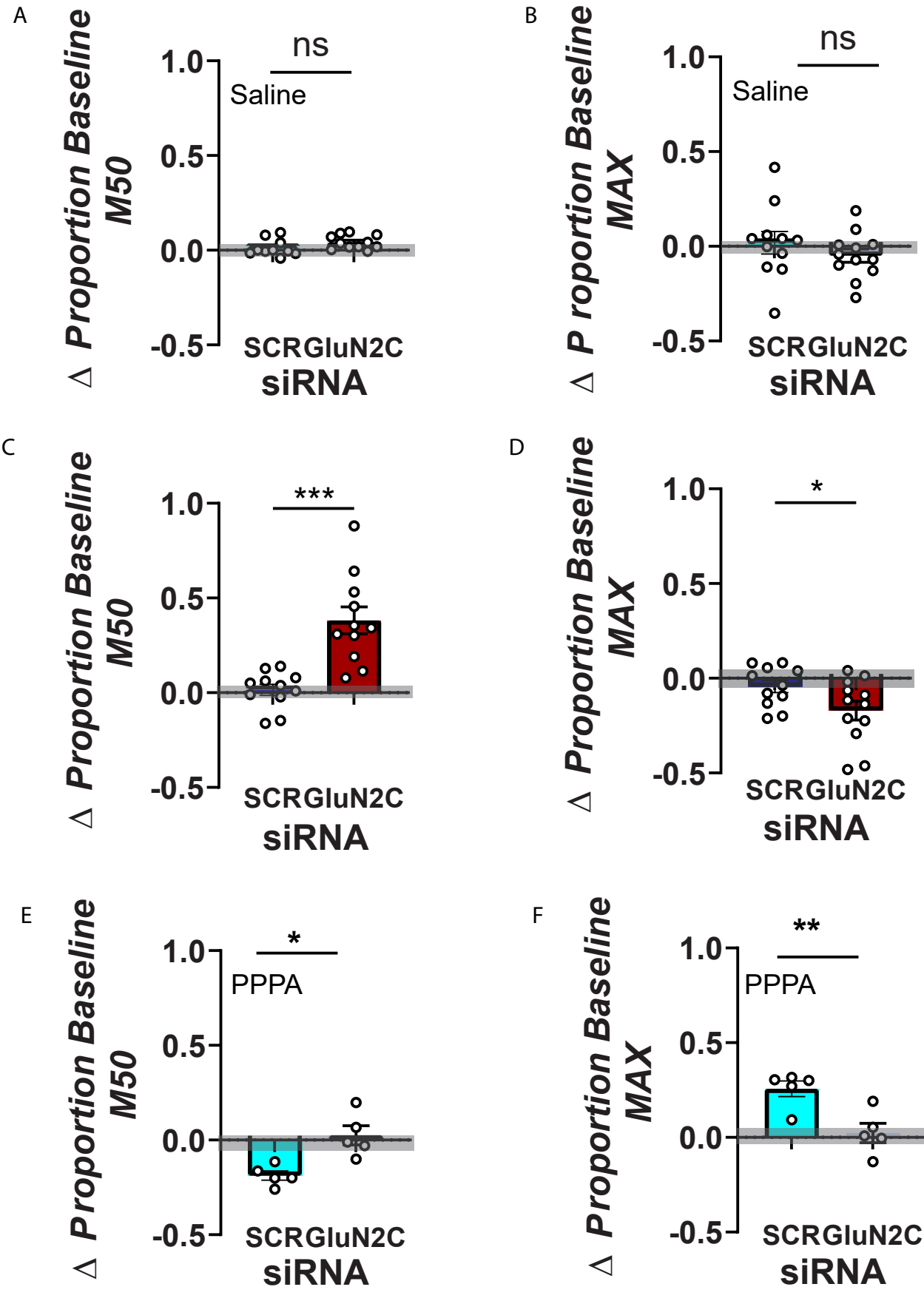
A
Δ Proportion Baseline M50
ns
Saline
1.0
0.5
0.0
-0.5
SCRGluN2C
siRNA
B
Δ P roportion Baseline MAX
ns
Saline
1.0
0.5
0.0
-0.5
SCRGluN2C
siRNA
C
Δ Proportion Baseline M50
***
1.0
0.5
0.0
-0.5
SCRGluN2C
siRNA
D
Δ Proportion Baseline MAX
*
1.0
0.5
0.0
-0.5
SCRGluN2C
siRNA
E
Δ Proportion Baseline M50
*
PPPA
1.0
0.5
0.0
-0.5
SCRGluN2C
siRNA
F
Δ Proportion Baseline MAX
**
PPPA
1.0
0.5
0.0
-0.5
SCRGluN2C
siRNA